

UDK 661.183.8;549.613.4

Microstructure Development and Phase Evolution of Alumina-mullite Nanocomposite

A. Sedaghat¹, E. Taheri-Nassaj^{1*}, G.D. Soraru², T. Ebadzadeh³

¹Department of Materials Science and Engineering, Tarbiat Modares University, PO Box 14115-143, Tehran, Iran

²Department of Materials Engineering and Industrial Technology, University of Trento, Via Mesiano 77, 38050 Trento, Italy

³Materials & Energy Research Centre, PO Box 14155-4777, Tehran, Iran

Abstract:

In this work, alumina-mullite composites (5-15 vol.%) were prepared using sol-gel derived alumina composite nanopowders. The results revealed the formation of intragranular and intergranular mullites inside and between the alumina grains, respectively. Accordingly, the intragranular mullites (average grain size, 0.3 μm) were smaller than the intergranular mullites (average grain size, 0.5 μm). Moreover, the alumina grains (average grain size, 1.0 μm) are larger than the mullites. Meanwhile, the mullites showed positive results in the prevention of the alumina grains growth and the retardation of densification. The relative density of alumina-15 vol.% mullite that was sintered at 1650 °C for 2 h, was obtained as 98.7 %. After sintering at 1750 °C for 2 h, the mullite was decomposed.

Keywords: Phase evolution; Microstructure development; Alumina; Mullite; Nanocomposite.

1. Introduction

Alumina has found different applications such as insulating refractory linings of furnaces, seals, thermocouple wire protection and armors because of its physical and mechanical properties (high melting point and high strength) [1-3]. On the other hand, mullite in the alumina matrix reduces the Young's modulus and thermal expansion coefficient of the composite, leading to a better thermal shock resistance [4-6]. Meanwhile, mullite has low toughness and hardness [7]. Small mullite additions (5–15 vol.%) allow desirable values of hardness and toughness of alumina to be maintained while reducing the Young's modulus below that of alumina, so that it is expected that the thermal shock behaviour will be improved [8].

A number of recent works have involved the addition of impurities in order to achieve better densification behaviour and, as a consequence, higher densities and better microstructures and mechanical properties [9, 10]. Schehl et al. [11] presented a modified processing route which consists in the doping of a commercial high-purity alumina powder so that its microstructure is modified with such nanoparticles as zirconia and mullite, formed at the sintering stage. As a result, the grain boundaries of the high-purity alumina powder are modified by segregation of the secondary phases or by the formation of well-distributed zirconia and mullite nanoparticles. Thus it should be possible to tailor microstructures by

*) Corresponding author: taheri@modares.ac.ir

means of secondary phases by referring to the corresponding phase equilibrium diagrams. Very high homogeneous multicomponent ceramics and composite ceramics can be obtained via sol-gel method, since the energy and, therefore, the synthesis temperature of this method is low [12].

In this work, alumina-mullite composites (5-15 vol.%) were prepared using sol-gel derived alumina composite nanopowders, with the ultimate aim to investigate the positioning of mullite and its effect in the microstructure of the alumina-mullite composite. Meanwhile, the phase evolution of this composite was studied.

2. Experimental

The flowchart of the procedure is shown in Fig. 1. The alumina composite nanopowders (Fig. 2, Tab. I) were synthesized by sol-gel method using aluminum chloride hexahydrate (Merck 101084) dissolved in distilled water and tetraethyl orthosilicate (Sigma-Aldrich 131903) dissolved in absolute ethanol. Based on the stoichiometric ratio ($3\text{Al}_2\text{O}_3 \cdot 2\text{SiO}_2$) and the desired volume percentage (0, 5, 10, 15 vol.%) of mullite, the aqueous solution of salt with the required amount of the alcoholic solution of tetraethyl orthosilicate (TEOS) was refluxed at 60°C for 24 h. After condensation, the gel was dried at 120°C for 24 h and ground in an agate mortar. The precursors of the alumina and the alumina-mullite composites were calcined at 900°C for 2 h and subsequently attrition-milled with high purity alumina balls and absolute ethanol for 1 h. After drying, the powders were sieved using a $80\ \mu\text{m}$ mesh. The powders were uniaxially pressed under 38 MPa. Then they were cold isostatically pressed (CIP) at 380 MPa, and finally sintered in air at 1650°C for 2 h. Moreover, the alumina-15 vol.% mullite specimens were sintered at 1300, 1500, 1650 and 1750°C for 2 h to investigate their microstructure development.

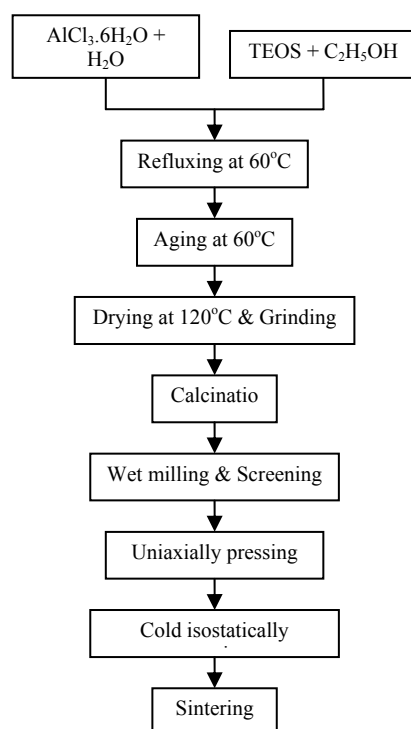


Fig. 1. The flow chart of the processing of Alumina–Mullite nanocomposite

Tab. I Properties of the alumina – 15 vol. % mullite precursor calcined at 900°C for 2h

BET surface area [m ² /g]	105.4 ± 0.4
Apparent density [g/cm ³]	3.646 ± 0.007
Mean particle size [nm]	15
Surface area of pores [m ² /g]	106
Total pore volume [cm ³ /g]	0.50
Average pore diameter (4V/A by BET) [nm]	19.0

X-ray diffraction (XRD) was carried out for phase characterization of the alumina and the alumina-mullite composites (5, 10 and 15 vol.%) sintered at 1650 °C for 2 h. The phase evolution of the alumina-15 vol.% mullite, thermally treated at different temperatures (400-1750 °C), was studied by XRD. The XRD patterns were recorded in the range of $10 < 2\theta < 80$ using Philips X-pert model with Cu K α .

The microstructure of the sintered bodies was studied by a XL 30, Field Emission Environmental Scanning Electron Microscope (FEI-Philips) equipped with a Link Energy Dispersive X-ray system. The specimens for SEM were polished to a 1 μ m surface finish using diamond spray. Thereafter, they were thermally etched for 1 h at 100 °C below the sintering temperature. The average grain size was defined as the average apparent diameter of the grains determined directly by using image analysis software. Moreover, the average length and width of the grains were measured on the elongated grains.

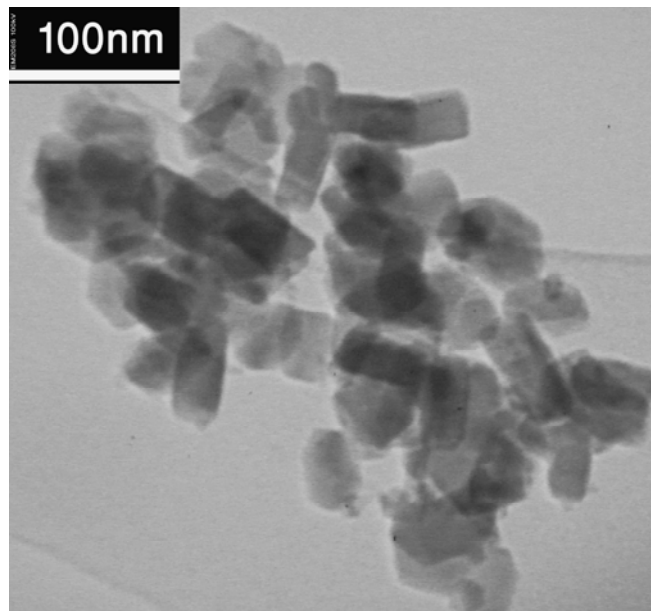


Fig. 2. The TEM micrograph (bright field) of alumina-15 vol.% mullite precursor calcined at 900°C for 2h (average particle size, 31 nm)

Powder morphology and microstructure characterization of the sintered specimens was performed by transmission electron microscopy (TEM) employing a Philips CM12 instrument, while the instrument was operated at 120 KV. The bulk specimens were prepared following the standard grinding and ion-polishing procedures.

The Archimedes method [13] was used in this work to measure the density of the samples sintered by using distilled water as an immersion medium and determining three

mass values (dry, suspended and saturated masses). Moreover, the relative density was calculated by dividing the bulk density to the theoretical density of the specimen.

3. Results and discussion

As shown in Fig. 3, the alumina and the alumina-mullite composites were prepared with the desired amounts of mullite (5, 10 and 15 vol.%) after sintering at 1650 °C for 2 h. This assumption was supported by a modified Rietveld method [14]. The microstructures of these samples are shown in Fig. 4(a-d). Fig. 4 depicts a reducing of the grain size of both alumina and mullite by increasing mullite content. The average grain size of alumina-0, 5, 10 and 15 vol.% mullite (Fig. 4) is 1.6, 1.3, 0.9 and 0.8 μm , respectively. Accordingly, the addition of tetraethyl orthosilicate to the alumina composite precursor has positive results in the prevention of the alumina grain growth.

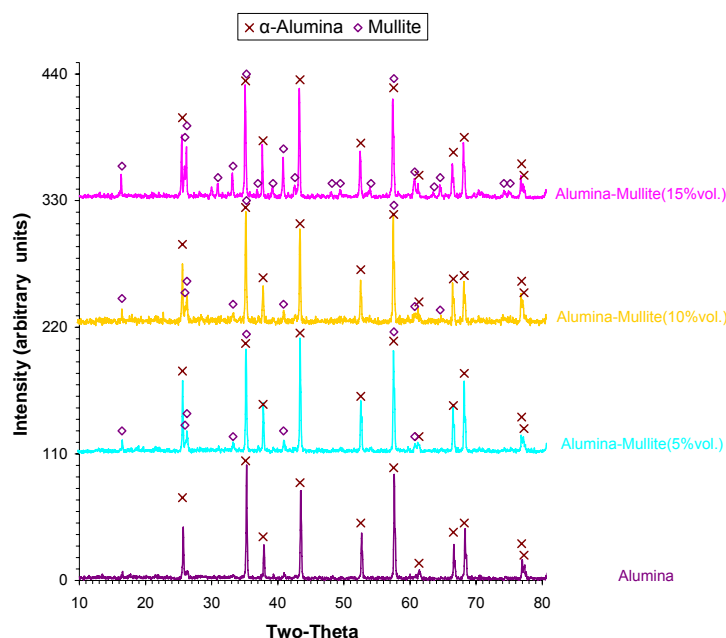
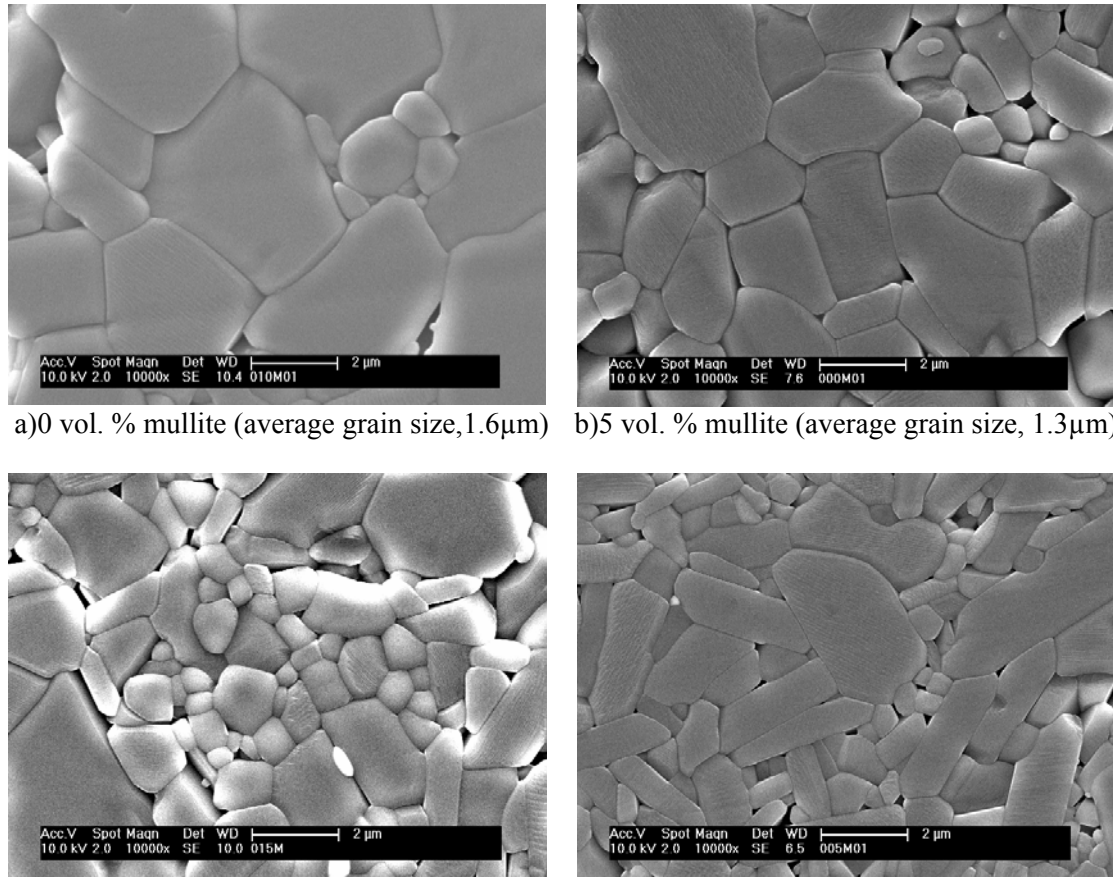


Fig. 3. The XRD patterns of alumina-mullite composites sintered at 1650 °C for 2 h

The microstructure of the alumina-10 vol.% mullite composite in BSE (Backscattered electrons) mode is shown in Fig. 5. The EDAX analyses of light areas (Point A) reveal the Aluminum (Al) and Oxygen (O) peaks and the EDAX analyses of dark areas (Point M) depict the Al, O and Si peaks. On the other hand, the XRD patterns of these samples (Fig. 3) reveal both alumina and mullite. So the light and dark areas are alumina and mullite, respectively. Fig. 5 depicts that the intergranular mullite has been formed between the alumina grains and the intragranular mullite has been formed inside the alumina grain.

Schehl et al. [11] prepared alumina composites from powder-alkoxide mixtures (alpha alumina powder with $d_{50} = 0.46 \mu\text{m}$ and tetraethyl orthosilicate). They presented a microstructure of the alumina composite, after sintering at 1600 °C for 2 h, with a mean grain size of 1.88 μm and the mullite phase (dark areas) located at the triple points, not inside the alumina grains. Fig. 6 shows the TEM micrograph (bright field) of the sintered alumina-5 vol.% mullite composite at 1650 °C for 2 h and the EDAX analysis of point M. Also a spherical mullite particle with 190 nm diameter was observed inside one of the alumina grains. The size of the intragranular mullite (average particle size, 0.3 μm) is lower than that

of the intergranular mullite (average grain size, 0.5 μm) and the intergranular mullite grains are smaller than the alumina grains (average grain size, 1.0 μm).



a) 0 vol. % mullite (average grain size, 1.6 μm) b) 5 vol. % mullite (average grain size, 1.3 μm)
 c) 10 vol. % mullite (average grain size, 0.9 μm) d) 15 vol. % mullite (average grain size, 0.8 μm)

Fig. 4. The FESEM micrographs (SE Mode) of alumina-mullite composites sintered at 1650°C for 2h

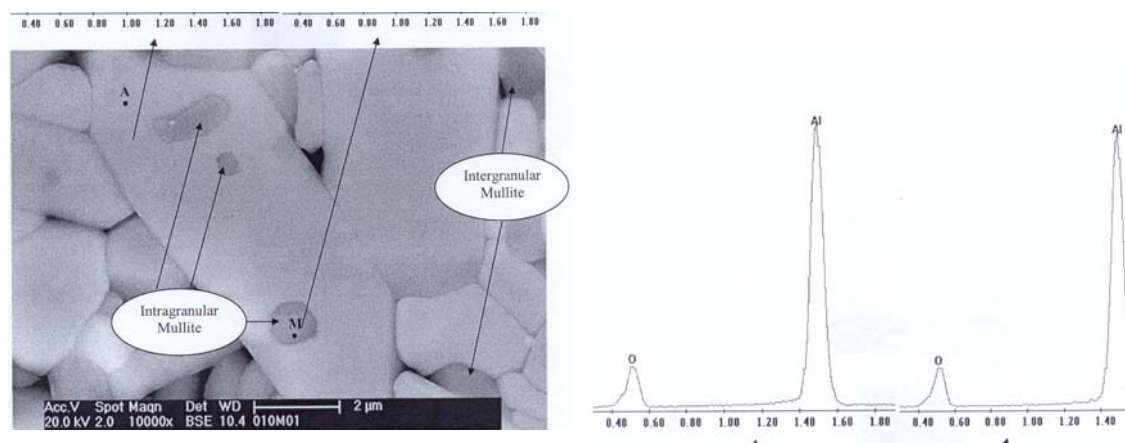


Fig. 5. The FESEM micrograph (BSE Mode) of alumina-10 vol.% mullite composite sintered at 1650°C for 2h and the EDAX analysis of points A and M (A: Alumina, M: Mullit)

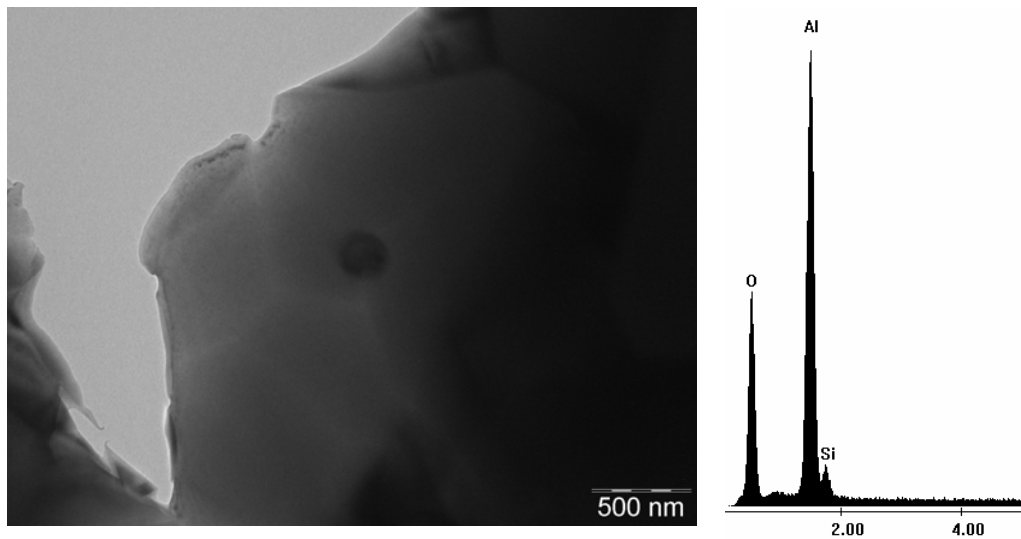


Fig. 6. The TEM micrograph (bright field) of alumina-5 vol.% mullite composite sintered at 1650°C for 2h and the EDAX analysis of point M

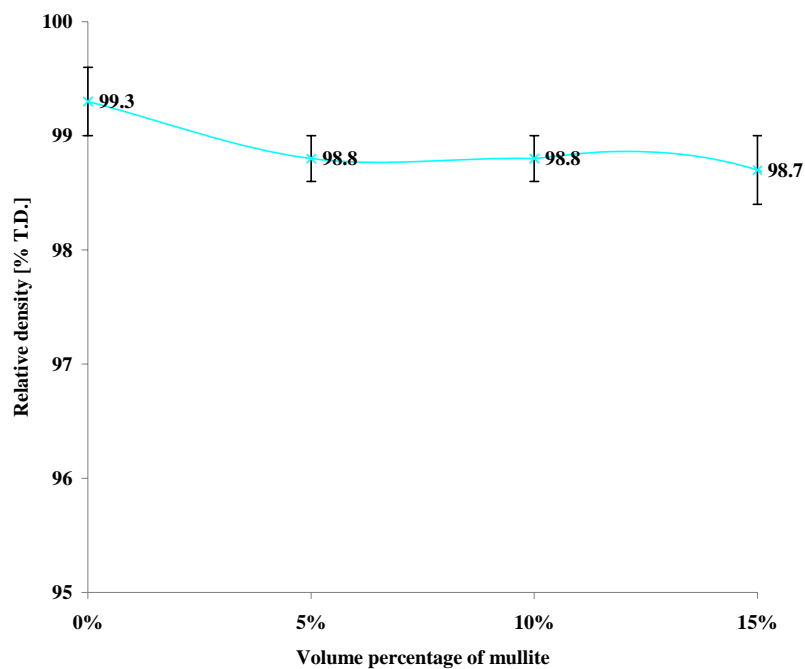


Fig. 7. The relative densities of alumina and alumina-mullite composites after being sintered at 1650°C for 2h

Fig. 7 shows the densification of alumina and alumina composites after sintering at 1650 °C for 2 h. The relative density of the alumina after sintering was obtained as 99.3 ± 0.3 %T.D., which was reduced to 98.7 ± 0.3 %T.D. in the presence of mullite. By increasing of the volume percentage of mullite, the rate of densification was retarded a little.

In another work [15], an alumina mat was prepared by sol-gel technique using aluminum chloride hexahydrate with different amounts of colloidal silica (0, 2, 4, 6 and 8 wt.% SiO₂). The transitional alumina was transformed into alpha alumina at 1000 °C, and by increasing the silica content, this phase transformation was retarded to 1200 °C. Fig. 7 presents the XRD patterns of the alumina-15 vol.% mullite that was thermally treated at different temperatures (400 – 1750 °C). Moreover, it reveals that the transitional alumina [16]

was transformed into alpha alumina [17] at 1000 °C and the source of SiO₂ was tetraethyl orthosilicate, not colloidal silica. So it is supposed that the phase transformation was not retarded due to the dissolution of tetraethyl orthosilicate. The mullite peaks [18] were detected by increasing the sintering temperature.

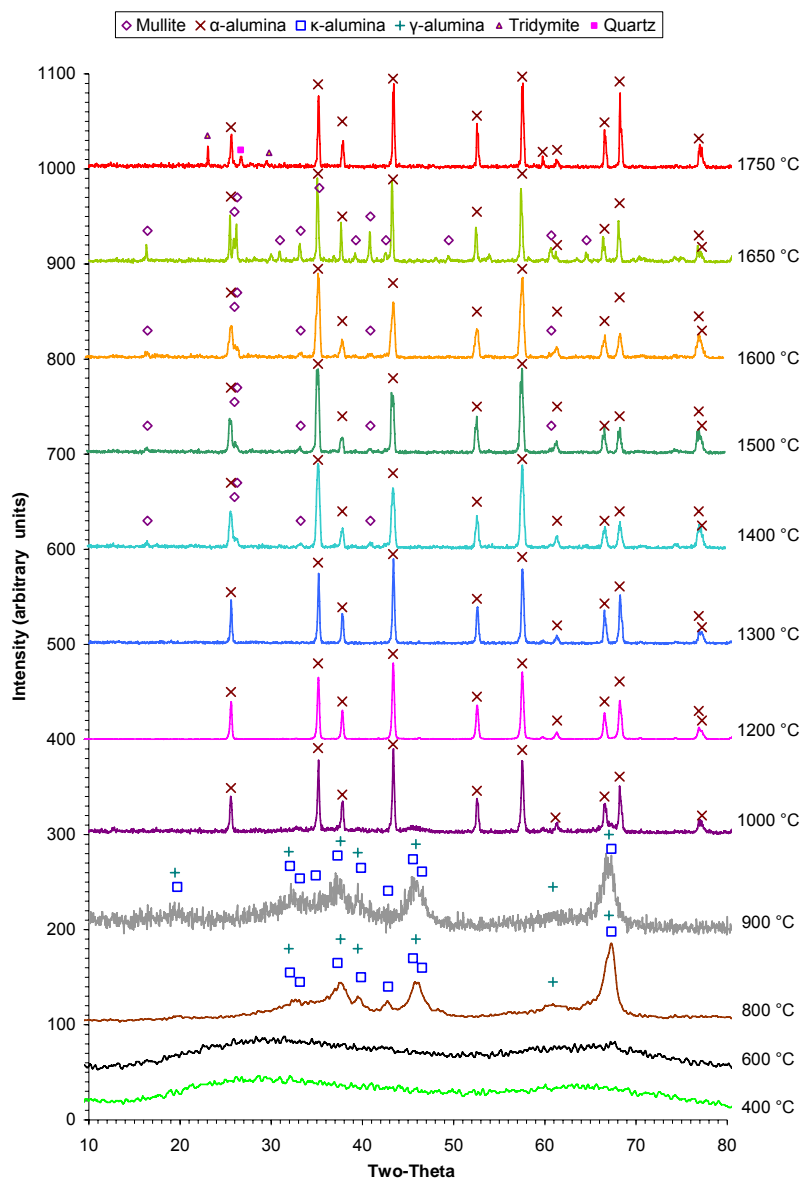
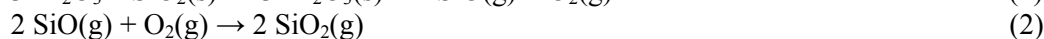
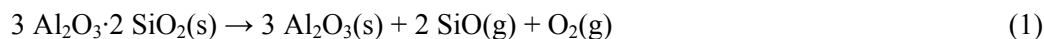
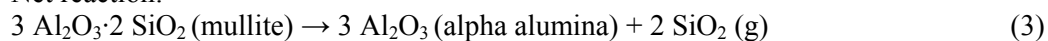


Fig. 8. The XRD patterns of alumina-15 vol.% mullite precursor calcined at different temperatures (400-1750°C)

The XRD pattern of the alumina-15 vol.% mullite that was thermally treated at 1750 °C for 2 h (Fig. 8) depicts alpha alumina peaks [17] and some peaks of quartz [19] and tridymite [20]. Decomposition of mullite has been reported at high temperature in reducing atmospheres [21]. For example, mullite specimen surfaces had heat-treated in helium between 1650 and 1800 °C, degrade with the formation of alpha alumina and volatile silicon species, so that the recession progresses from the surface towards the bulk of specimens. So it can be supposed that in the samples of this work, the mullite was decomposed at 1750 °C by the following reactions [21]:



Net reaction:



s = solid, g = gaseous

The microstructure of alumina-15 vol.% mullite composite that was sintered at 1750 °C for 2 h (Fig. 9) reveals a grain growth. Meanwhile, the average grain size was calculated as 2.2 μm at 1750 °C. The micrograph was taken in BSE mode to investigate the phase evolution. There are dark and light areas. The EDAX analyses (Fig. 9 (b, c)) and XRD pattern (Fig. 8) of these areas revealed that the silica particles (dark areas) are embedded in the alumina grains (light areas) at 1750 °C.

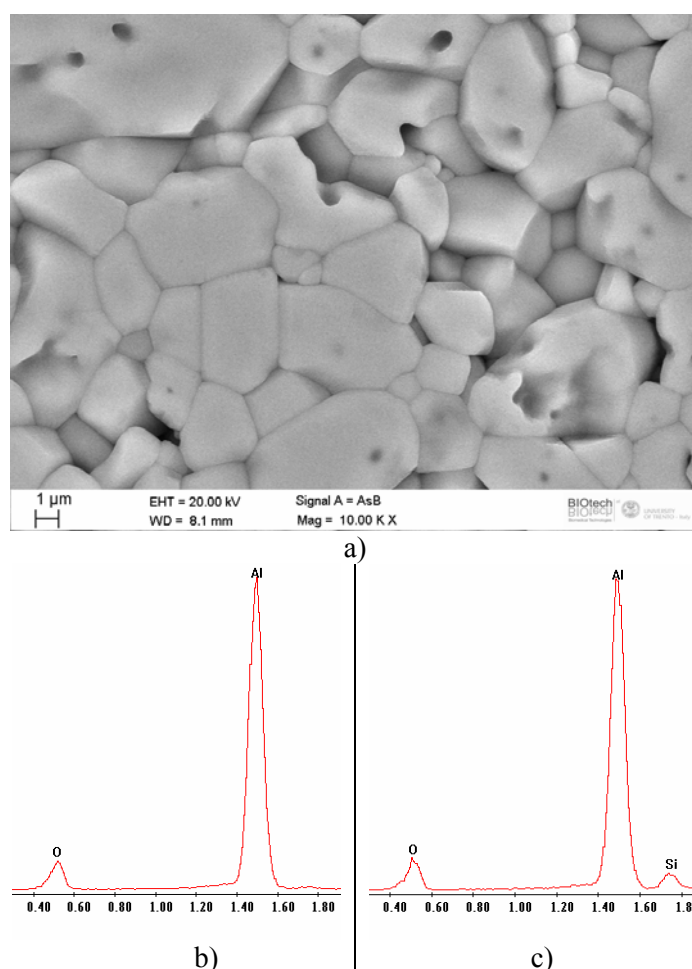


Fig. 9. The FE-SEM micrograph (BSE Mode) of alumina-15 vol.% mullite composite sintered at 1750 °C for 2 h (a) with the EDAX analysis of light (b) and dark (c) areas (99.3 % T.D., average grain size, 2.2 μm)

Moreover, some pores are observed due to sintering or mullite decomposition. In addition, the TEM micrograph (bright field) and EDAX analysis of alumina-15 vol.% mullite composite that has been sintered at 1750 °C for 2 h are observed in Fig. 10. The presence of silica in the fracture edge is revealed by the EDAX analysis of point S (Fig. 10) and its XRD pattern (Fig. 8). There is also another pore with 300 nm diameter due to sintering or mullite decomposition.

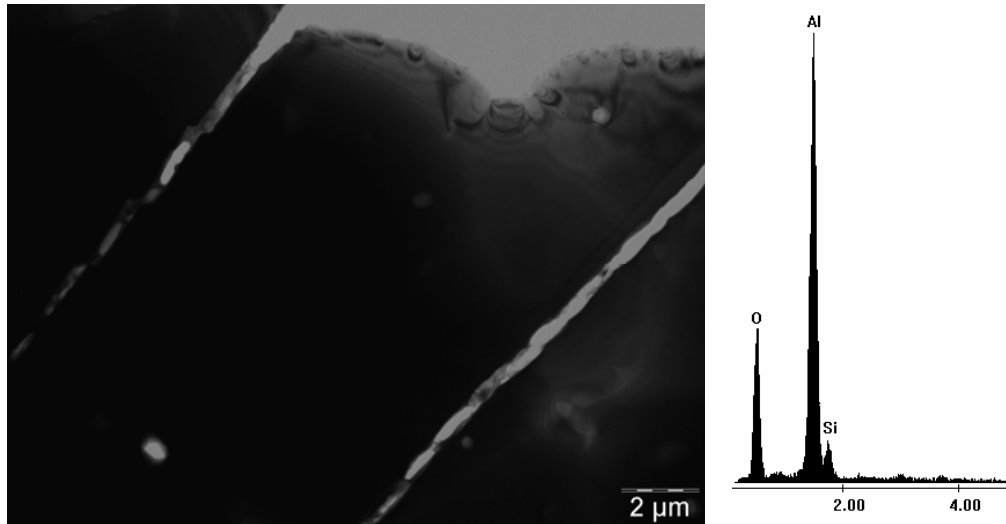


Fig. 10. The TEM micrograph (bright field) of alumina-15 vol.% mullite composite sintered at 1750 °C for 2 h and EDAX analysis of point S

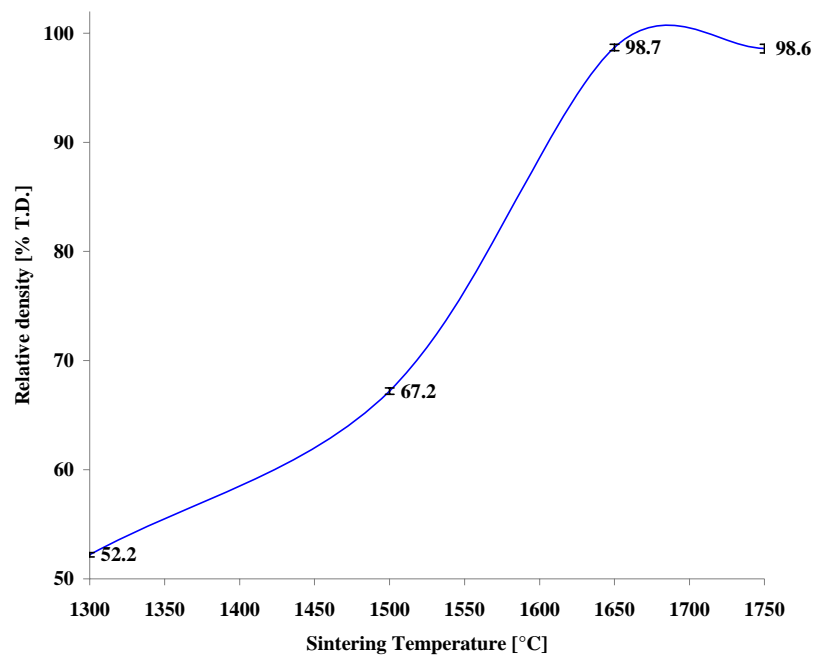


Fig. 11. The relative densities of alumina-15 vol.% mullite after being sintered at 1300-1750°C for 2h

Fig. 11 shows the densification of alumina-15 vol.% mullite after being sintered at different temperatures (1300-1750 °C) for 2h. After sintering, the relative density increased by increasing of the temperature (Fig. 11). At 1500, 1650 and 1750 °C, the relative densities were calculated as 67.2 ± 0.3 , 98.7 ± 0.3 and 98.6 ± 0.4 , respectively. At 1500 °C, the densification was not completed and at 1750 °C, the mullite was decomposed according to Fig. 7. So it was preferred to sinter at 1650 °C.

4. Conclusions

In this work, the alumina composite nanopowders, synthesized via sol-gel method using aluminum chloride hexahydrate and tetraethyl orthosilicate, were used to prepare the alumina-mullite composite by pressing, CIP and sintering. The findings are summarized as follows:

1. The intergranular mullite was formed between the alumina grains while the intragranular mullite was formed inside the alumina grains.
2. The grain size of the intragranular mullite (average grain size, 0.3 μm) is lower than that of the intergranular mullite (average grain size, 0.5 μm). Moreover, that of the intergranular mullite is lower than that of the alumina (average grain size, 1.0 μm).
3. The mullite showed positive results in the prevention of the alumina grain growth and also in the retardation of densification.
4. The relative density of alumina-15 vol.% mullite sintered at 1650 $^{\circ}\text{C}$ for 2h, was calculated as 98.7 %.
5. After sintering at 1750 $^{\circ}\text{C}$ for 2 h, the mullite was decomposed and some pores were observed due to sintering or mullite decomposition.

Acknowledgement

The authors wish to thank Francesco Tassarolo (section of Electron Microscopy, Department of Medicine Laboratory-APSS Trento) for FE-SEM microstructural characterizations.

5. References

1. Richerson D.W. Modern ceramic engineering, M. Dekker, (1992), pp. 808-823
2. Medvedovski E. Alumina–mullite ceramics for structural applications. *Ceram Int* 32 (2006), 369–375
3. Luo H.H., Zhang F.C., Roberts S.G. Wear resistance of reaction sintered alumina/mullite composites. *Mat Sci Eng A* 478 (2008),270–275
4. Mezquita S., Uribe R., Moreno R., Baudín C. Influence of mullite additions on thermal shock resistance of dense alumina materials Part 2: Thermal properties and thermal shock behaviour. *Br Ceram Trans* 100(6) (2001), 246-250
5. Aksel C. The effect of mullite on the mechanical properties and thermal shock behaviour of alumina–mullite refractory materials. *Ceram Int* 29 (2003), 183–188
6. Zhang F.C., Luo H.H., Roberts S.G. Mechanical properties and microstructure of Al_2O_3 /mullite composite. *J Mater Sci* 42 (2007), 6798–6802
7. Aksel C. The role of fine alumina and mullite particles on the thermomechanical behaviour of alumina–mullite refractory materials. *Mater Lett* 57 (2002), 708–714
8. Moreno R., Mezquita S., Baudín C. Influence of mullite additions on thermal shock resistance of dense alumina materials Part 1: Processing studies. *Br Ceram Trans* 100(6) (2001), 241-245
9. Thompson AM, Soni KK, Chan HM, Harmer MP, Williams DB, Chabala JM, Levi-Scotti R. Dopant distributions in rare-earth-doped alumina. *J Am Ceram Soc* 80(2) (1997), 373–6
10. Fang J., Thompson AM, Harmer MP, Chan HM. Effect of yttrium and lanthanum on the final-stage sintering behavior of ultrahigh-purity alumina. *J Am Ceram Soc* 80(8) (1997), 2005–12

11. Schehl M., Díaz L.A., Torrecilla R. Alumina nanocomposites from powder-alkoxide mixtures. *Acta Mater* 50(2002), 1125–1139
12. Won C.W., Siffert B. Preparation by sol-gel method of SiO₂ and mullite (3Al₂O₃·2SiO₂) powders and study of their surface characteristics by inverse gas chromatography and zetametry. *Colloid Surface A: Physicochemical and Engineering Aspects* 131(1998), 161-172
13. ‘Standard Test Method for Water Absorption, Bulk Density, Apparent Porosity, and Apparent Specific Gravity of Fired Whiteware Products’, ASTM Designation: C 373 – 88, ASTM Standards, Vol. 15.02, 2005.
14. Lutterotti L., Ceccato R., Dal Maschio R., Pagani E. *Mater Sci Forum* 87(1998), 278-281
15. Sedaghat A., Taheri-Nassaj E., Naghizadeh R. An alumina mat with a nano microstructure prepared by centrifugal spinning method. *J Non-Cryst Solids* 352 (2006), 2818-2828
16. Powder Diffraction File, Card No. 10-0425, JCPDS
17. Powder Diffraction File, Card No. 10-0173, JCPDS
18. Powder Diffraction File, Card No. 15-0776, JCPDS
19. Powder Diffraction File, Card No. 01-087-2096, JCPDS
20. Powder Diffraction File, Card No. 01-085-0419, JCPDS
21. Schneider H., Komarneni S. Mullite. WILEY-VCH Verlag GmbH and Co. KGaA, Weinheim, (2005), pp. 236-237

Садржај: У овом раду, алумина-мулитни композити (5-15 vol.%) су припремљени сол-гел методом из нанометарских композита алумине. Резултати указују на формирање интра и интер-грануларних мулитних структура унутар и између зрна алумине, истим редом. Сходно томе, интрагрануларни мулити (просечне величине зрна 0,3 μm) су мањи од интергрануларних мулита (просечна величина зрна 0,5 μm). Даље, зрна алумине (просечне величине зрна 1,0 μm) су већа од мулитних. У међувремену, мулити показују позитивне резултате у превенцији раста зрна алумине и престанак денсификације. Релативна густина алумина-15 vol.% мулита која је синтерована на 1650 °C 2 h, је била 98,7 %. Након синтеровања на 1750 °C 2 h, мулит се разградио.

Кључне речи: еволуција фаза; развој микроструктуре; алумина; мулит; нанокмозити.
